International Journal of Advanced Mechanical Engineering.
ISSN 2250-3234 Volume 8, Number 1 (2018), pp. 251-262

http://www.ripublication.com

CFD Analysis of Semi-Circular Rib Roughened Solar Air Heater

Yadaba Mahanand [1], Abhijit Mahato [2] and Debanshu Shekhar Khamari[3]

[1]Government College of Engineering Kalahandi,
[2]Abacus Institute of Engineering and Management, Mogra,

[3]Government College of Engineering Kalahandi,

ydb.gcek2016@gmail.com, mahatoa79@gmail.com, debanshushekhar@gmail.com

Abstract:

The 2D heat transfer and fluid flow phenomenon through an artificially roughened solar air heater is investigated by means of a numerical model at a constant heat flux of 1000 W/m^2. A modern CFD code ANSYS FLUENT v 14.5 is used to simulate fluid flow and heat transfer through the solar air heater. The duct wall, Absorber plate and roughness materials are assumed to be homogeneous & isotropic and also the thermal conductivity is independent of temperature. The present work show that the Renormalization-group k-epsilon model provides the results close to those, worked out from available empirical co-relation for two-dimensional steady flow solar air heaters. The maximum enhancement of average Nusselt number has been found to be 2.3104 times that of smooth duct for relative roughness pitch of 7.14 and for relative roughness height of 0.042.

Keywords: CFD Analysis; Absorber plate; Solar air heaters; Nusselt number; Friction factor; Reynolds number.

Nomenclature:

D	Hydraulic diameter of duct, mm
P_h	Wetted perimeter, mm
A	Cross-sectional area, m^2
h	Heat transfer coefficient, W/m^{2}K
k	Thermal conductivity of air, W/mK
m	Mass flow rate, kg/s
f	Friction factor

N_u Nusselt number

P_r Prandtl number

R_e Reynolds number

L1 Entrance length of duct, mm

L2 Test length of duct, mm

L3 Exit length of duct, mm

W Width of duct, mm

H Depth of duct, mm

e Rib height, mm

P Rib Pitch, mm

W/H Duct aspect ratio

I. INTRODUCTION AND LITERATURE SURVEY

Solar air heaters with artificial roughness in the form of fine wires of different shapes, sizes and orientations on the underside of the absorber plate is one of the important and effective design improvement that have been proposed to improve the thermal performance. Artificial roughness has been used to enhance the heat transfer coefficient by creating turbulence in the flow. However it would also result in an increase in friction losses and hence greater pumping power requirements for air through the duct. In order to keep the friction losses at a low level, the turbulence must be created only in the region very close to the duct surface .i.e. in the laminar sub-layers.

The concept of artificial roughness was first applied by Joule [1] to enhance heat transfer coefficients for in-tube condensation of steam and since then many experimental investigations were carried out on the application of artificial roughness in the areas of cooling of gas turbine, electronic equipment, nuclear reactors, and compact heat exchangers etc. Nunner [2] was the first who developed a flow model and likened this model to the temperature profile in smooth tube flow at increased Prandtl number. The proposed flow model predicts that roughness reduces the thermal resistance of the turbulence dominated wall region without significantly affecting the viscous region. A friction correlation for flow over sand-grain roughness was developed by Nikuradse. Based on law of the wall similarity, Nikuradse [3] presented the pressure drop results in terms of roughness function R and roughness Reynolds number e+. Dipprey and Sabersky [4] developed a heat-momentum transfer analogy relation for flow in a sand-grain roughened tube and achieved excellent correlation of their data. The concept proposed by Dipprey and Sabersky was so common and it can be applied to any roughness for which law of the wall similarity holds. Prasad and Mullick [5] were the first who introduced the application of artificial roughness in the form of small diameter wire attached on the underside of absorber plate to improve

the thermal performance of solar air heater for drying purposes.

II. CFD INVESTIGATION:

The CFD code ANSYS ANSYS FLUENT v 14.5 has been used to simulate fluid flow and heat transfer, and also to solve the various conservation equations for mass, momentum and energy. Computational domain, mesh generation, governing equations, boundary conditions, selection of suitable turbulence model and solution procedure is discussed in details to the following sub-sections.

a. Computational domain

The computational domain (2D model) design and simulation for the study of artificial roughness in solar air heater is in accordance with the ASHRE 93-2003. According to these standard entire flow field is divided into three sections i.e. Entry section, Test section and Exit section respectively. The first section is the entry section and is provided so that the flow will be fully developed before test section. The exit section which is provided to make sure that the effect of flow exit is not affecting the test section. The geometric model developed for current study is as shown below.

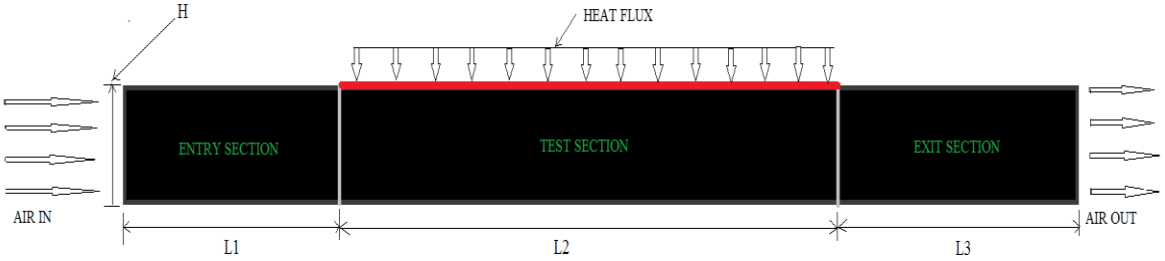

Fig. 1 Computational domain for smooth absorber plate solar air heater

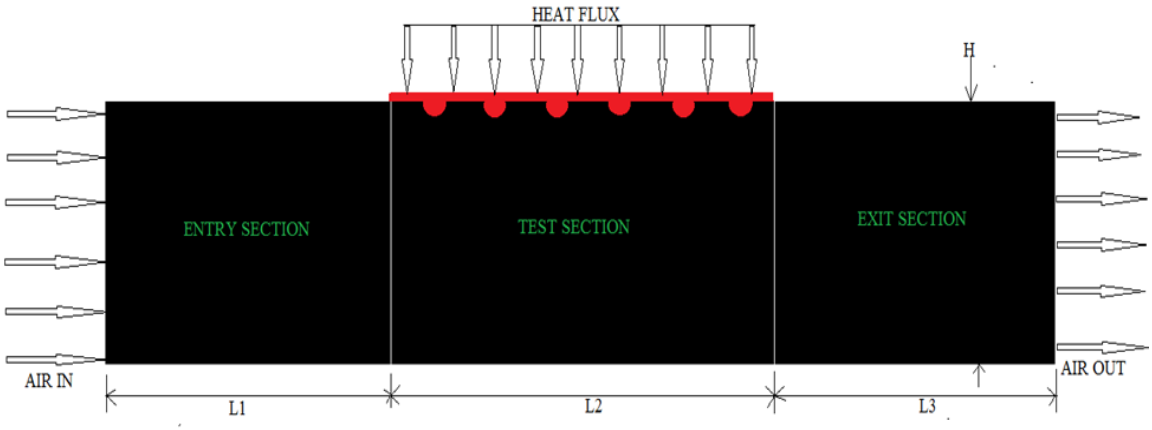

Fig. 2 Computational domain for roughened absorber plate solar air heater

Table 1 Geometrical and operating parameters for computational analysis

Entrance length of duct, L1	225mm
Test length of duct, L2	121mm
Exit length of duct, L3	115mm
Width of duct, W	100mm
Depth of duct, H	20mm
Hydraulic diameter of duct, D	33.33mm
Duct aspect ratio, W/H	5
Rib height, e	0.7mm,1mm,1.4mm
Rib Pitch, P	10mm,15mm,20mm,25mm
Reynolds number, Re	3800,5000,8000,12000,15000,18000

b. Mesh generation

Non-uniform grids are generated for all numerical simulations performed in this work. Non-uniform grids are commonly used in modeling when large gradients are expected, local details are desired, or complex geometries are encountered. Automatic (patch conforming) non-uniform grids are generated for all numerical simulations performed in this work. Grids are generated using ANSYS ICEM CFD V14.5 software. A non-uniform mesh with very fine mesh size is used to resolve the laminar sub-layer and is shown in fig.2. Since low-Reynolds-number turbulence models are employed, the grids are generated so as to be fine. Present non-uniform quadrilateral mesh contained 95,483 quad cells with cell size of

0.2mm. This size is suitable to resolve the laminar sub-layer. For grid independence test, the number of cells is varied from 54,272 to 1, 93,288 in five steps.

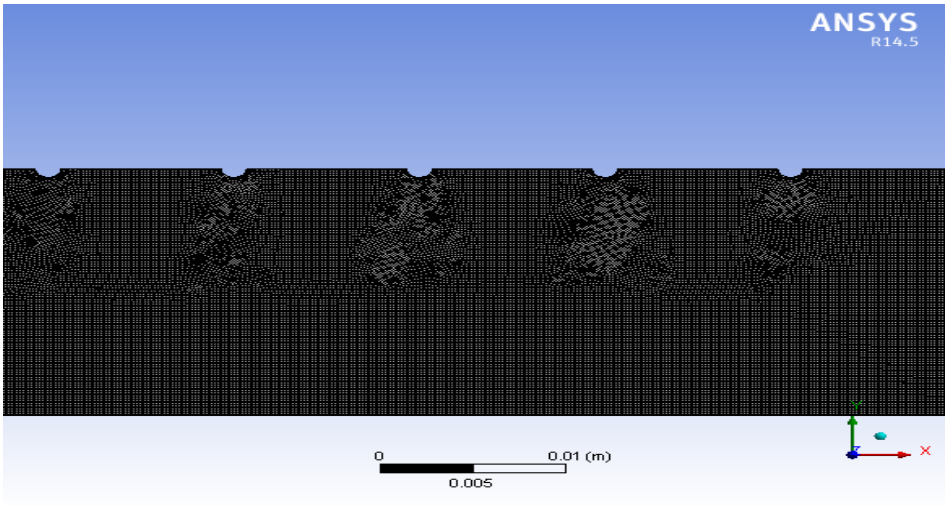

Fig. 3 2D closed mesh view

c. Governing Equation

The phenomenon of flow for an artificially roughened solar air heater duct is ruled by the steady 2-dimensional form of continuity, Navier-Stokes equation and energy equation. In Cartesian co-ordinate system these equations can be written as

(i) Continuity Equation:-

$$\frac{\partial}{\partial x_i}(\rho u_i) = 0 \tag{2.1}$$

(ii) Momentum Equation:-

$$\frac{\partial}{\partial x_i}(\rho u_i u_j) = -\frac{\partial p}{\partial x_i} + \frac{\partial}{\partial x_j}\left[\mu\left(\frac{\partial u_i}{\partial x_j} + \frac{\partial u_j}{\partial x_i}\right)\right] + \frac{\partial}{\partial x_j}(-\rho u_i' u_j') \tag{2.2}$$

(iii) Energy Equation:-

$$\frac{\partial}{\partial x}(\rho u_j T) = \frac{\partial}{\partial x_j}\left(\left(\Gamma + \Gamma_t\right)\frac{\partial T}{\partial x_j}\right) \tag{2.3}$$

Where Γ and Γ_t are molecular thermal diffusivity and turbulent thermal diffusivity, respectively and are given by

$$\Gamma = \frac{\mu}{Pr} \quad \text{And} \quad \Gamma_t = \frac{\mu_t}{Pr_t} \tag{2.4}$$

d. Boundary Condition

The inlet velocity of the flow is calculated by using Reynolds number. The outlet boundary condition is specified at the exit of the computational domain. At exit outlet boundary condition is applied atmospheric pressure (1.013 x 10^5 Pa). Table 2 shows the Thermo-physical properties of air and aluminium absorber plate. Table 3 shows Boundary condition of study domain.

Table 2 Thermo-physical properties of air and aluminium absorber plate for computational analysis

Properties	**Working fluid (air)**	**Absorber plate (aluminium)**
Density (ρ) (kg/m^3)	1.225	2719
Specific heat (Cp) (J/kg-K)	1006.43	871
Thermal conductivity (k) (W/m//K)	0.0242	202.4
Viscosity (μ) (N/m^2)	1.7894*10^{-5}	-

Table 3 Boundary condition of study domain

Surface	Boundary Condition	Value
Inlet	Inlet Velocity	Calculated from Re
Outlet	Outlet Pressure	Atmospheric Pressure
Top Surface	Absorber plate	Heat Flux of 1000w/m^2
Bottom Surface	Wall	Insulated

III. RESULTS AND DISCUSSIONS

a. Validation of CFD model

The selection and validation of turbulence model is carried out by comparing the Nusselt number predicted by different turbulence model such as standard k-ε model, Renormalized group k-ε model (RNG) with empirical correlation available for smooth duct of the solar air heater i.e. Dittus-Boelter correlation.

Fig.4 compare the variation of Nusselt number with Reynolds number using different turbulence model and results obtained from Dittus-Boelter empirical correlation for a smooth duct of solar air heater. For low Reynolds number (relevant in solar air heater), it has been observed that the results obtained by the Renormalization Group (RNG) k- ε model are good agreement with the Dittus-Boelter empirical correlation results. This ensures the accuracy of the numerical data obtained from the present work.

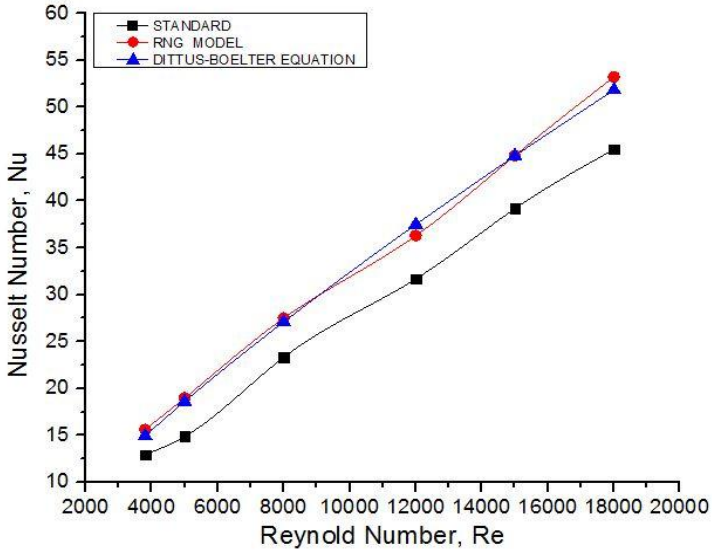

Fig.4 Comparison between Nusselt number predictions using different turbulence model with Dittus-Boelter correlation for smooth duct.

The Table 4 and 5 show that how the Nusselt Number enhancement factor changes with respect to Reynolds number for different values of P/e and e/D ratio and the Friction factor enhancement ratio Respectively which is predicted from CFD investigation.

Table 4 Nusselt number Enhancement ratio predicted by CFD analysis

	Nusselt Number Enhancement Ratio						
e/D	P/e	Re=3800	Re=5000	Re=8000	Re=12000	Re=15000	Re=18000
0.021	14.29	1.4511	1.479023	1.4941	1.52389	1.53817	1.5553
	21.43	1.42059	1.450298	1.47569	1.50008	1.52878	1.52412
	28.57	1.40889	1.43339	1.4546	1.47278	1.511668	1.4582
	35.71	1.35732	1.402158	1.408824	1.44639	1.46037	1.4084
0.03	10	1.783717	1.795978	1.8328	1.8560	1.87398	1.8848
	15	1.7387	1.76789	1.7865	1.8162	1.85109	1.8656
	20	1.71795	1.7415688	1.7452	1.77809	1.8291	1.8378
	25	1.6378	1.6767	1.70185	1.7401	1.8075	1.819
0.042	7.14	2.2097	2.2531	2.2674	2.2739	2.29067	2.3104
	10.71	2.08654	2.10907	2.1799	2.19483	2.05073	2.17555
	14.29	2.0334	2.0732	2.1193	2.1384	2.0336	2.1009
	17.85	1.980	2.0335	2.0906	2.0906	2.0437	2.0708

Table 5 Friction factor enhancement ratio predicted from CFD investigation

	Friction factor enhancement ratio						
e/D	P/e	Re=3800	Re=5000	Re=8000	Re=12000	Re=15000	Re=18000
0.021	14.29	2.1624	2.5155	2.0964	2.0679	2.10447	1.946378
	2.43	2.14018	2.13638	2.0594	2.0437	2.0918	2.1109
	28.57	2.121158	2.0932	1.96439	1.97802	2.0439	1.90656
	35.71	2.0573	2.00255	1.867588	1.9192	2..001195	1.8681
0.03	10	2.548878	2.5219	2.5055	2.2876	2.4591	2.439
	15	2.50901	2.50172	2.47435	2.4783	2.4677	2.4486
	20	2.48368	2.47407	2.4449	2.4575	2.4491	2.4235
	25	2.4322	2.41705	2.41099	2.41959	2.3986	2.38069
0.042	7.14	3.1206	3.1087	3.07156	3.04832	3.01409	3.01297
	10.71	2.7015	2.6714	2.6651	2.6593	2.124427	2.5740
	14.29	2.4459	2.42563	2.4734	2.4703	1.8856	2.323
	17.85	2.350	2.309	2.502	2.3679	2.13093	2.2552

The effect of Relative roughness pitch P/e on Heat transfer has been shown typically in Fig.5 and Fig.6. Fig.5 (a, b and c) shows that the Nusselt number increases with increase in Reynolds number for all cases. It can be seen from Fig6 (a, b and c) shows that the Nusselt number as a function of Relative roughness pitch (P/e) for different values of Reynolds number and for fixed (a) e/D=0.021,(b)e/D=0.03 and (c)e/D=0.042. It can be seen that for a given Relative roughness height Nusselt number decreases with an increase in Relative roughness pitch. This is due to fact that with the increase in Relative roughness pitch number of reattachment point reduces. The maximum enhancement of average Nusselt number has been found to be 2.3104 times that of smooth duct for relative roughness pitch of 7.14 and for relative roughness height of 0.042.

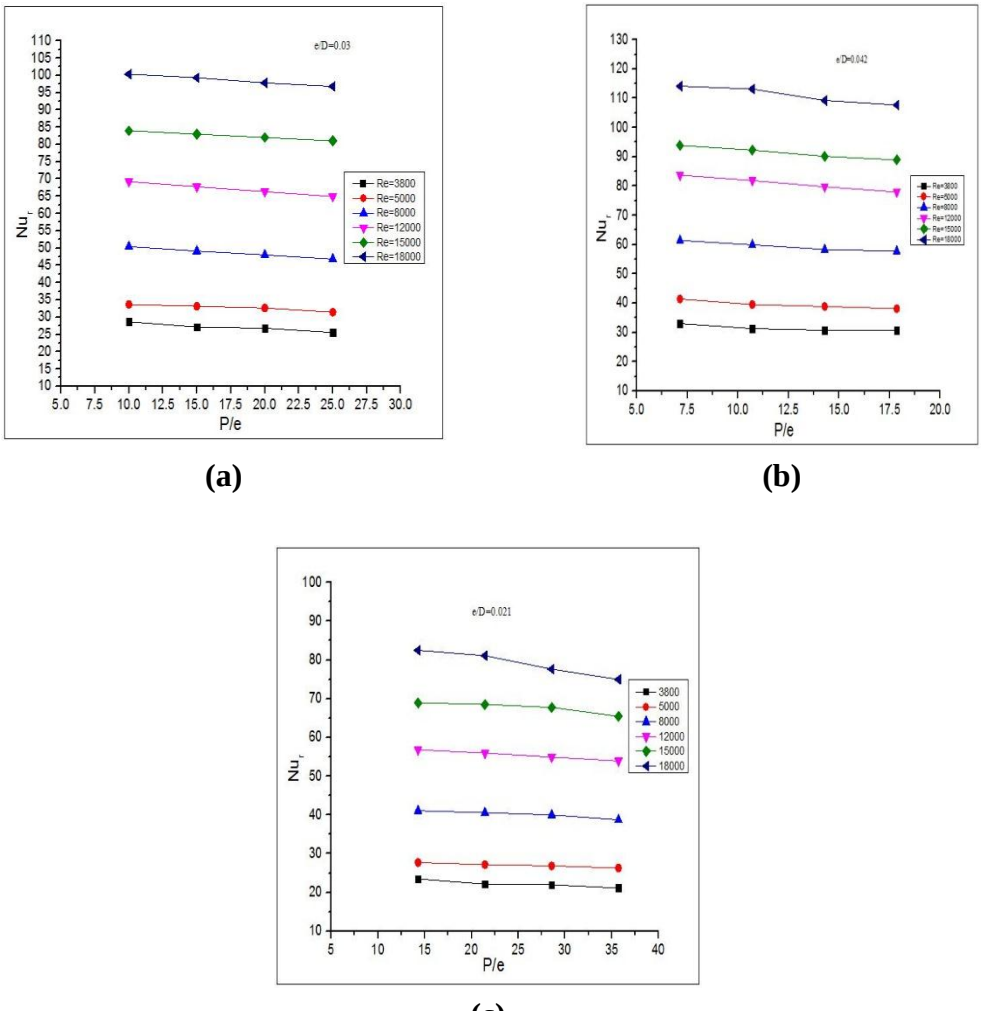

Fig 5 (a, b and c) Nusselt number as a function of Relative roughness pitch (P/e) for different values of Reynolds number for fixed (a) e/D=0.021, (b)

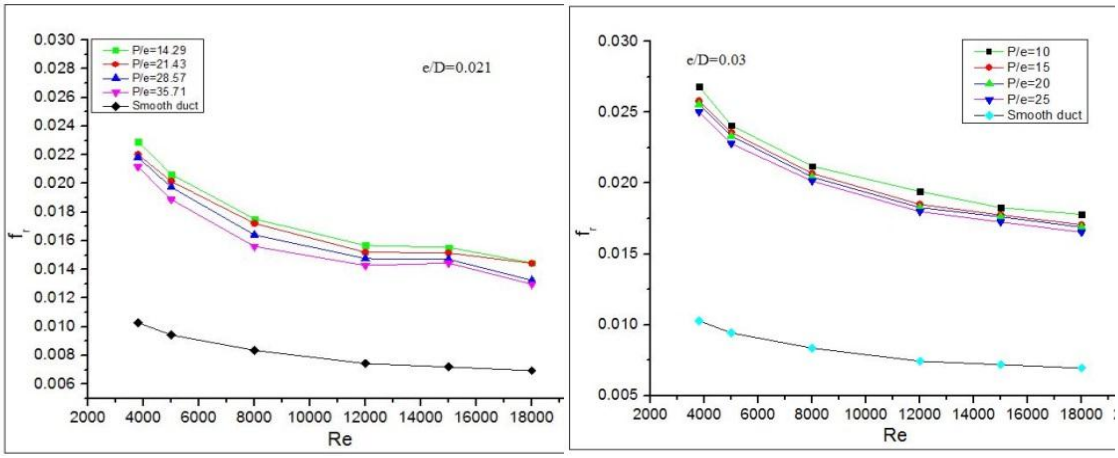

(a) (b)

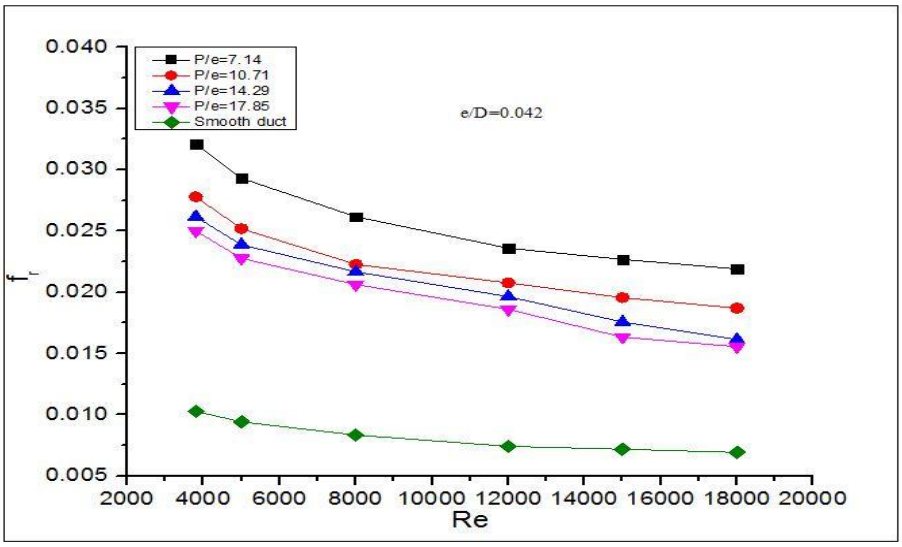

(c)

Fig 6 (a, b and c) Friction factor as a function of Reynolds number for different values of P/e and for fixed (a) e/D=0.021, (b) e/D=0.03 and (c) e/D=0.042.

It is found that thermal enhancement factor value vary between 1.1 to 1.65 for the range of parameter investigated. It is observed that roughened duct having semi-circular rib with e/d=0.042 and P/e=14.29 gives the better thermal enhancement factor for the studied range of Reynolds number. Fig 6 shows that the variation of thermal enhancement factor with Reynolds number for all cases

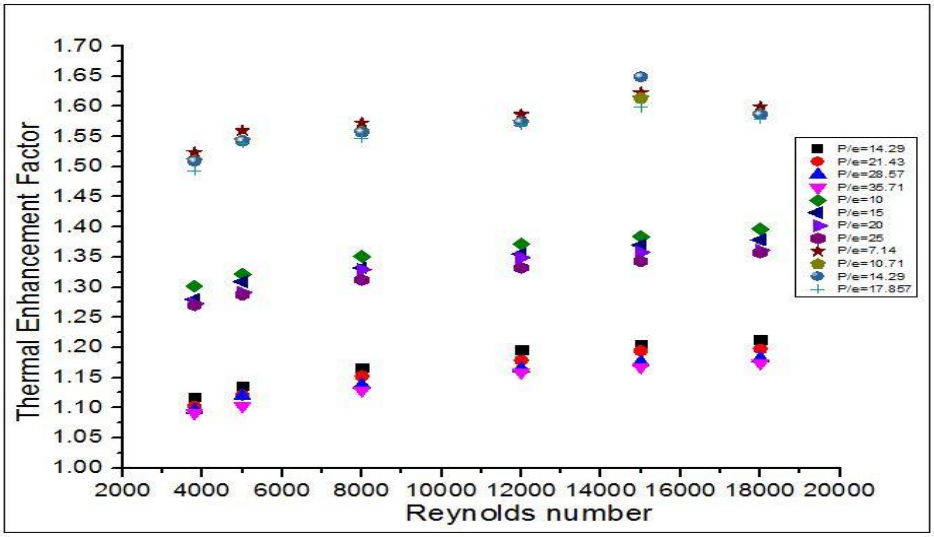

Fig.7 variation of Thermal Enhancement factor with Reynolds number for different values of relative roughness height (e/D) and relative roughness pitch (P/e).

b. Validation of results

Fig. 8 shows the validation of present analysis of artificially roughened solar air heater having semi-circular rib roughness.

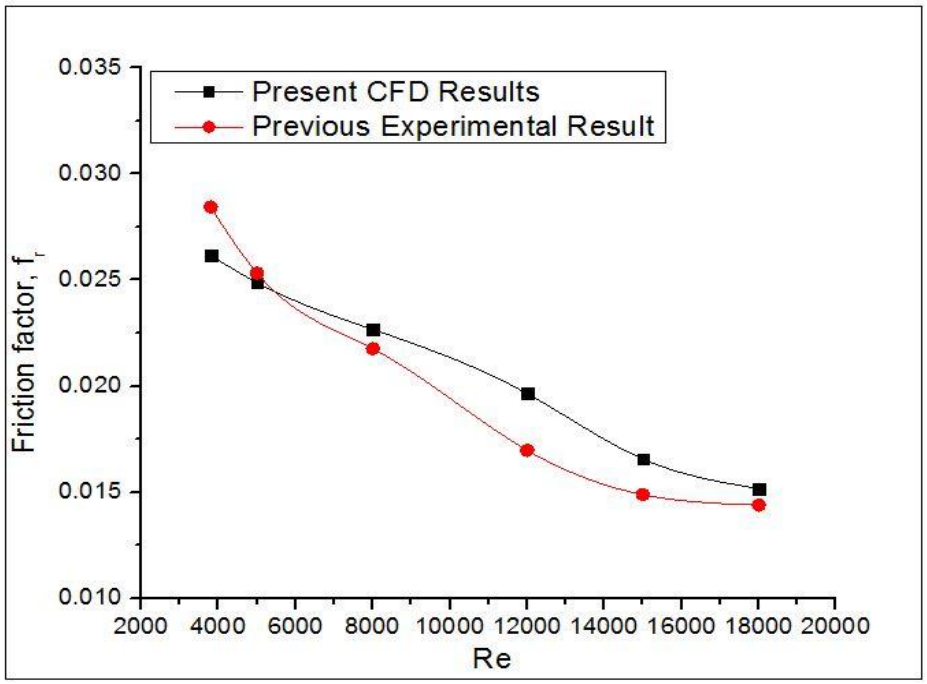

Fig. 8 Comparison between present CFD result and previous experimental result which was carried out in Circular rib roughened solar air heater under similar flow condition

Table 6. Compares the operating parameters range with previous accepted range

Widely accepted numerical results	Shape of ribs	Range
Yadav and Bhagoria(14)	Circular transverse wire rib	P/e=10.71 and e/D=0.042
Yadav and Bhagoria(15)	Square sectioned rib	P/e=10.71 and e/D=0.042
Chaube et al.	Rectangular sectioned rib	P/e=13.33 and e/D=0.042
Present CFD study	Semi-circular sectioned rib	P/e=14.29 and e/D=0.042

IV. CONCLUSION

The effects of Reynolds number, relative roughness pitch and relative roughness height on the heat transfer and fluid flow process are discussed. Key findings from the study are as follows:

1. The Renormalization-group (RNG) k-epsilon turbulence model predicted very close results to the experimental results, which yields confidence in the predictions done by numerical analysis in the present study.
2. The maximum enhancement of average Nusselt number has been found to be 2.3104 times that of smooth duct for relative roughness pitch of 7.14 and for relative roughness height of 0.042.
3. The maximum enhancement of average friction factor has been found to be 3.12 times that of smooth duct for relative roughness pitch of 7.14 and for relative roughness height of 0.042. The maximum enhancement of average friction factor occurs at a Reynolds number of 3800.

REFERENCES

[1] J.P. Joule,"On the surface condensation of steam", Philosophical Transactions of the Royal Society of London, 151:133-60; 1861

[2] W. Nunner,"Heat transfer and pressure drop in rough pipes", vol. 22. VDI-Forsch, 1956, 445-B, English Trans, AERE Lib / Trans; 786; 1958.

[3] J. Nikuradse,"Laws of flow in rough pipes", NACA Technical Memorandum, 1292; 1950.

[4] D.F. Dippery, R.H. Sabersky,"Heat and momentum transfer in smooth and rough tubes at various Prandtl number", International Journal of Heat and Mass Transfer, 6:329-53; 1963.

[5] K. Prasad, S.C. Mullick,"Heat transfer characteristics of a solar air heater used for drying purposes", Applied Energy, 13(2):83-93; 1983.

[6] R. Karw, S.C. Solanki, J.S. Saini,"Thermo-hydraulic performance of solar air heaters having integral chamfered rib roughness on absorber plates", Energy, 26:161-76; 2001.

[7] R.P. Saini, J. Verma,"Heat transfer and friction factor correlations for a duct having dimple-shaped artificial roughness for solar air heaters", Energy, 33; 1277-87; 2008.

[8] S. Singh, S. Chander, J.S. Saini,"Heat transfer and friction factor correlations of solar air heater ducts artificially roughened with discrete V-down ribs", Energy, 36:5053-64; 2011.

[9] J.L. Bhagoria, J.S. Saini, S.C. Solanki,"Heat transfer coefficient and friction factor correlations for rectangular solar air heater duct having transverse wedge shaped rib roughness on the absorber plate", Renewable Energy, 25:341-69; 2002.

[10] B.E. Launder, D.B. Spalding, Lectures in Mathematical Models of Turbulence, Academic Press, London, England, 1972.

[11] V.S. Hans, R.P. Saini, J.S. Saini, Heat transfer and friction factor correlations for a solar air heater duct roughened artificially with multiple V-ribs, Sol. Energy 84 (2010), 898e911.

[12] M. Sethi, Varun, N.S. Thakur, Correlations for solar air heater duct with dimpled shape roughness elements on absorber plate, Sol. Energy 86 (2012) 2852e2861.

[13] B. E. Launder, and D. B. Spalding, Lectures in Mathematical Models of Turbulence, Academic Press, London, 1972.

[14] S. V. Patankar, Numerical Heat Transfer and Fluid Flow, Hemisphere, Washington, D.C. 1980.

[15] S. W. Ahn, The Effects of Roughness Types on Friction Factors and Heat Transfer in Roughened Rectangular Duct, Int. Comm. in Heat and Mass Transfer, vol. 28, no. 7, pp. 933–942, 2001.

[16] A. Chaube, P. K. Sahoo, and S. C. Solanki, Analysis of Heat Transfer Augmentation, and Flow Characteristics due to Rib Roughness over Absorber Plate of a Solar Air Heater, Renewable Energy, vol. 31, pp. 317–331, 2006.

[17] Prasad BN, Saini JS. Effect of artificial roughness on heat transfer and friction factor in a solar air heater. Solar Energy 1988;41(6):555e60.